VIROLOGICA SINICA 2016, 31 (4): 314–323
DOI: 10.1007/s12250-016-3723-7

RESEARCH ARTICLE

Identification and characterization of two cleavage fragments from the *Aquareovirus* nonstructural protein NS80

Qingxiu Chen[1,2], Jie Zhang[1], Fuxian Zhang[1], Hong Guo[1], Qin Fang[1]✉

1. State Key Laboratory of Virology, Wuhan Institute of Virology, Chinese Academy of Sciences, Wuhan 430071, China
2. University of the Chinese Academy of Sciences, Beijing 100039, China

***Aquareovirus* species vary with respect to pathogenicity, and the nonstructural protein NS80 of aquareoviruses has been implicated in the regulation of viral replication and assembly, which can form viral inclusion bodies (VIBs) and recruit viral proteins to its VIBs in infected cells. NS80 consists of 742 amino acids with a molecular weight of approximately 80 kDa. Interestingly, a short specific fragment of NS80 has also been detected in infected cells. In this study, an approximately 58-kDa product of NS80 was confirmed in various infected and transfected cells by immunoblotting analyses using α-NS80C. Mutational analysis and time course expression assays indicated that the accumulation of the 58-kDa fragment was related to time and infection dose, suggesting that the fragment is not a transient intermediate of protein degradation. Moreover, another smaller fragment with a molecular mass of approximately 22 kDa was observed in transfected and infected cells by immunoblotting with a specific anti-FLAG monoclonal antibody or α-NS80N, indicating that the 58-kDa polypeptide is derived from a specific cleavage site near the amino terminus of NS80. Additionally, different subcellular localization patterns were observed for the 22-kDa and 58-kDa fragments in an immunofluorescence analysis, implying that the two cleavage fragments of NS80 function differently in the viral life cycle. These results provide a basis for additional studies of the role of NS80 played in replication and particle assembly of the *Aquareovirus*.**

KEYWORDS ***Aquareovirus*; nonstructural protein NS80; cleavage fragments; subcellular localization; functional analysis**

INTRODUCTION

Viruses belonging to the family *Reoviridae* are currently classified into 15 genera and can infect a wide variety of organisms, including vertebrates, invertebrates, and plants. These viruses are non-enveloped and contain a genome with 9–12 segments enclosed within a multiple protein-shelled core. Aquareoviruses isolated from aquatic animals, including finfish and crustaceans, are classified into seven species (*Aquareovirus A* to *Aquareovirus G*) based on their genome identities (Mertens et al., 2011). Generally, aquareoviruses are minimally pathogenic in aquatic cultures. However, Grass carp reovirus (GCRV, a member of *Aquareovirus C*) can cause fatal epidemic hemorrhagic disease in fingerling and yearling grass carp, and has been regarded as the most highly pathogenic aquareovirus (Rangel et al., 1999). Therefore, GCRV serves as an ideal model for studying the replication and pathogenesis of aquareoviruses.

Similar to the structure of other reoviruses in the family *Reoviridae*, GCRV virion is a multilayered icosahedral symmetry with 12 pentameric turrets that reside on the surface of the core or at the five-fold axis of the intact particle (Cheng et al., 2008; Zhang et al., 2010). The eleven-segmented double-stranded RNA genome encodes 7 structural proteins (VP1–VP7) and 5 nonstruc-

Received: 11 January 2016, Accepted: 5 May 2016,
Published online: 6 June 2016
✉Correspondence:
Phone: +86-27-87198551, Fax: +86-27-87198551,
Email: qfang@wh.iov.cn
ORCID: 0000-0003-4681-0060

tural proteins (NS16, NS26, NS31, NS38, and NS80) (Attoui et al., 2002). The viral core that serves as a transcriptase particle *in vivo* is composed of 5 proteins (VP1–VP4 and VP6), and also possesses transcriptional activity *in vitro* (Smith et al., 1980; Yang et al., 2012; Yan et al., 2014). VP5 and VP7 make up the outer capsid required for viral entry into host cells during infection (Zhang et al., 2010). In addition, the nonstructural proteins are involved in the viral replication cycle (Fan et al., 2009a; Fan et al., 2010; Cai et al., 2011; Shao et al., 2013; Yan et al., 2015). Phylogenetic and three-dimensional structural analyses have revealed that there is a close evolutionary relationship between aquareoviruses and orthoreoviruses, including mammalian orthoreoviruses (MRV) and avian reoviruses (ARV) (Shaw et al., 1996; Attoui et al., 2002; Fang et al., 2005; Cheng et al., 2008; Cheng et al., 2010).

The replication and assembly of reoviruses occur in distinctive cytoplasmic viral inclusion bodies (VIBs), which contain double-stranded RNA, viral proteins, and both complete and incomplete particles (Silverstein et al., 1970; Fields et al., 1971; Brookes et al., 1993; Broering et al., 2004). VIBs are thought to provide a physical scaffold to concentrate viral components and related cellular factors so that viral replication and nascent particle assembly proceed at specific sites in the cytoplasm. A single μNS of MRV can form VIBs in transfected cells and can recruit five core structural proteins (λ1, λ2, λ3, μ2, and σ2), the nonstructural protein σNS, and cellular clathrin (Sharpe et al., 1982; Parker et al., 2002; Becker et al., 2003; Miller et al., 2003; Broering et al., 2004; Touris-Otero et al., 2004; Miller et al., 2010; Ivanovic et al., 2011). The nonstructural protein NS80 of GCRV, the analogue of the μNS protein of MRV and ARV, consists of 742 amino acids with a molecular weight of approximately 80 kDa (Fan et al., 2009b; Fan et al., 2010). Previous studies in our lab have demonstrated that NS80 can form VIBs in singly expressed or infected cells. In addition, NS80 can retain viral proteins (VP1–VP4 and VP6) in VIBs, and associate with the nonstructural protein NS38 and newly synthesized viral RNAs in infected cells (Shao et al., 2010; Shao et al., 2013; Yan et al., 2015). Additionally, the C-terminal regions, including His569 and Cys571, in the coiled-coil region of NS80 are crucial for VIB formation (Shao et al., 2013).

The μNS protein, which is encoded by the *M3* gene of MRV and ARV, expresses two isoforms in infected cells (Wiener et al., 1989; Touris-Otero et al., 2004). Similarly, a shorter fragment with NS80 expression has also been found in GCRV-infected cells (Fan et al., 2009b; Fan et al., 2010; Shao et al., 2013; Yan et al., 2015). These results suggest that NS80 presents different forms or structural conformations in infected cells to regulate viral replication and assembly at different life cycle stages. As a step toward understanding the role of NS80 in the viral life cycle, we characterized NS80 and its related fragment, including their subcellular localization.

MATERIALS AND METHODS

Cells, virus, and antibodies

Ctenopharyngodon idellus kidney (CIK) cells and fathead minnow (FHM) cells were grown at 28 °C in Eagle's Minimum Essential Medium (Invitrogen, Carlsbad, USA) and Medium 199 (M199; Gibco BRL, Rockville, USA), respectively, and both media were supplemented with 10% fetal bovine serum (FBS). BHK-21 (baby hamster kidney) cells and Vero cells were cultivated in Dulbecco's modified Eagle medium (Gibco BRL, Rockville, MD, USA) supplemented with 10% FBS. The GCRV-873 strain used in this study was maintained in our laboratory, and virus propagation was described previously (Fang et al., 1989).

The polyclonal antibody (pAb) against GCRV NS80 C-terminal amino acid sequences (aa 335–742), named α-NS80C, was generated in our laboratory and is described elsewhere (Fan et al., 2009b), and the pAb against NS80 (1–334), termed α-NS80N, was prepared following previous methods (Fan et al., 2009b). The mouse anti-FLAG monoclonal antibody (mAb) was purchased from Shanghai Genomics (Shanghai, China) and mouse mAb against β-actin was purchased from Santa Cruz Biotechnology (Santa Cruz, California, USA). Rabbit anti-poly-ubiquitination pAb was purchased from Proteintech Co. (Wuhan, China). Alkaline phosphatase-coupled goat anti-rabbit IgG or goat anti-mouse IgG were purchased from Sigma-Aldrich (St. Louis, USA) and Alexa Fluor 488 or 568 donkey anti-rabbit IgG (H+L) antibodies were purchased from Invitrogen Co.

Plasmids and site-directed mutagenesis to obtain mutant NS80

The recombinant plasmids pCI-neo-NS80, pCI-neo-NS80 (130–742), and pNS38-GFP-NSP5 were constructed previously (Shao et al., 2013). The plasmids with FLAG-tagged NS80 at the N-terminus (FLAG-NS80) and C-terminus (NS80-FLAG), pCI-neo-NS80 (1–190) and pCI-neo-NS80 (386–742), were built using pCI-neo-NS80 as a template and then cloned into the pCI-neo vector (Promega, Madison, USA). In addition, based on a bioinformatics analysis using PeptideMass (http://web.expasy.org/peptide_mass), three plasmids with mutated NS80 carrying Arg to Ala substitutions at residues 137, 194, and 219 were also generated. The three mutants were generated using the plasmid pCI-neo-NS80 as a template with the Site-directed Gene Mutagenesis Kit (Beyotime Company, Haimen, China). The mutagenic oligonucleotide primer pairs are shown in Table 1. The

Table 1. Primers used to construct recombinant plasmids

Name of plasmids[a]	Primers (5′ to 3′)[b]
pCI-neo-NS80(R137A)	F: GCTGACCTGGCCACTGCCCACGCTTCCCTGCC
	R: GGCAGGGAAGCGTGGGCAGTGGCCAGGTCAGC
pCI-neo-NS80(R194A)	F: CCACCCCCTCCCCCCGCCGTCGATGACCCGGC
	R: GCCGGGTCATCGACGGCGGGGGGAGGGGGTGG
pCI-neo-NS80(R219A)	F: CTCCCGTCGATGCCAGCCGCTTCTACTTCTAC
	R: GTAGAAGTAGAAGCGGCTGGCATCGACGGGAG

Notes: [a] Each plasmid expressed the indicated NS80 mutants. [b] The changed bases are underlined.

correctness of the recombinant plasmids was confirmed by sequencing (Invitrogen Biotechnology Inc., Shanghai, China).

Infection

GCRV infection with sensitive cells was performed as previously described (Fang et al., 1989). Briefly, CIK or FHM cells were plated one or two days in advance and infected with GCRV-873 virus stock at a multiplicity of infection (MOI) of 1–5. After 45 min of absorption, unabsorbed viruses were removed and cells were washed with phosphate-buffered saline (PBS, 137 mmol/L NaCl, 2.7 mmol/L KCl, 8.1 mmol/L Na_2HPO_4, 1.5 mmol/L KH_2PO_4; pH 7.3). They were further incubated with fresh medium supplemented with 2% FBS. The virus-infected cells were collected at various time points to detect NS80 protein expression by immunoblotting (IB) as described previously (Shao et al., 2013). The relative intensity of IB band was quantified using Image J software.

Transfection and immunofluorescence assay

The transfection with recombinant plasmids and immunofluorescence (IF) assay were conducted following established methods, as previously described (Guo et al., 2013). In brief, cells were transfected with the indicated plasmid DNA and Lipofectamine 2000 transfection reagent according to the manufacturer's instruction (Invitrogen). At 24-h post-transfection (p.t.), cells were fixed and subjected to fluorescence microscopy. Transfected cells were fixed for 20 min at room temperature in 4% paraformaldehyde, washed three times with PBS, and permeabilized for 10 min with 0.2% Triton X-100. They were then washed and blocked three times for 2 h at 37 °C in PBS containing 5% bovine serum albumin. Then, cells were incubated with primary antibodies at 37 °C for 2 h. Three washes were conducted and secondary antibodies were added. After incubation at 37 °C for another 1 h, cells were washed three times with PBS and stained with Hoechst for 5 min. Finally, samples were examined with an Olympus-IX51 inverted fluorescence microscope and images were obtained and processed using Adobe Photoshop (Adobe Systems, San Jose, USA).

IB analysis

For the IB analysis, both infected and transfected cell lysates were collected, pelleted, and resuspended in PBS before they were resolved by sodium dodecyl sulfate-polyacrylamide gel (SDS-PAGE). They were then transferred to polyvinylidene fluoride membranes using a semi-dry transfer cell (Bio-Rad, Hercules, CA, USA) for 45 min at 100 mA. Membranes were blocked with 5% bovine serum albumin and then incubated with NS80 pAbs or mouse anti-FLAG mAb as primary antibodies. Alkaline phosphatase-coupled goat anti-rabbit or goat anti-mouse IgG were used as the secondary antibodies. Finally, reactive bands were detected with nitroblue tetrazolium (NBT) /5-bromo, 4-chloro, 3-indolylphosphate (BCIP) alkaline phosphatase substrate solution.

RESULTS

An approximately 58-kDa fragment was detected in infected and transfected cells

In a previous immunological assay using α-NS80C in infected cells, we found that a short polypeptide exhibits NS80 expression (Fan et al., 2009b). However, whether the small fragment is related to NS80 expression in different infected cells and its precise molecular mass are unclear. To resolve these issues, additional infection and transfection experiments in various cell types were performed. Two specific protein bands were detected in virus-infected and transfected cells in an IB analysis with α-NS80C. As shown in Figure 1A, a specific band of approximately 80 kDa was detected in virus-infected cells, which corresponded to the expected size of NS80. A slightly shorter polypeptide with a molecular mass of approximately 58 kDa was also detected using α-NS80C. The two specific bands were also detected in transfected cells (Figure 1B). These results suggested that the 58-

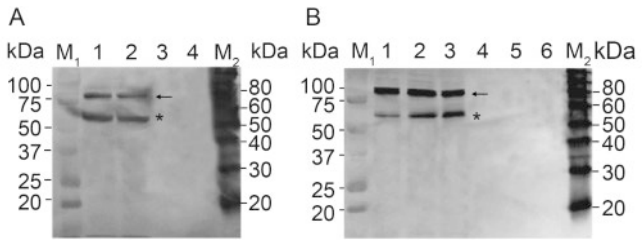

Figure 1. Analysis of NS80 expression in infected and transfected cells. Cell lysates were resolved by 10% SDS-PAGE, transferred to a PVDF membrane, and immunoblotted with α-NS80C. M, standard protein marker (M_1, Precision Plus Protein Dual Color Standards; M_2, Super-Signal Molecular Weight Protein Ladder). (A) Immunoblotting assay of NS80 expression in infected cells. Lanes 1–2, GCRV-infected FHM cells (lane 1) and CIK cells (lane 2); Lanes 3–4, mock-infected FHM cells (lane 3) and CIK cells (lane 4). (B) Immunoblotting assay of NS80 expression in transfected cells. Lanes 1–3, FHM (lane 1), BHK (lane 2) and Vero (lane 3) cells transfected with pCI-neo-NS80, respectively; Lanes 4–6, FHM (lane 4), BHK (lane 5) and Vero (lane 6) cells transfected with the pCI-neo empty vector, respectively. Arrow indicates the full-length NS80, and the asterisk indicates the 58-kDa NS80 fragment.

kDa fragment contains C-terminal amino acid sequences of NS80.

Three mutated protease-sensitive sites are not related to the 58-kDa fragment

Based on our initial assays, a 58-kDa fragment was detected with NS80 expression in infected and transfected cells. To determine whether the fragment resulted from transient protein degradation, a bioinformatics analysis was performed using PeptideMass (http://web.expasy.org/peptide_mass) (data not shown), and several arginine (R) protease sites were found in the N-terminal region of NS80. Based on the estimated size of the undefined polypeptide, three mutated NS80 constructs ($NS80^{R137A}$, $NS80^{R194A}$, and $NS80^{R219A}$) containing an Arg to Ala substitution at the N-terminus were constructed and then transfected into BHK cells. Previously constructed wild-type NS80 and deletion mutant NS80 (130–742) plasmids were used as controls in this assay (Shao et al., 2013). The expression of these mutants was confirmed by an IB analysis using α-NS80C. As shown in Figure 2A, a band corresponding to the full-length NS80 and a slightly shorter band were detected for the three missense mutants, indicating that the three mutated sites were not related to the 58-kDa fragment. To determine whether the three mutant proteins were substantially misfolded and targeted for degradation by the ubiquitin-proteasome system in transfected cells, colocalization assays for the three NS80 mutants using polyubiquitination antibody were performed. As shown in Figure 2B, none of the three mutant proteins appeared to be aggregated or strongly colocalized with conjugated ubiquitin in transfected cells. These results suggested that the three mutated sites in the N-terminal region of NS80 were unrelated to the 58-kDa fragment.

Infection time and dose influence the accumulation of the short NS80 fragment

After excluding the possibility that the short NS80 fragment was a transient product of protein degradation, the expression of NS80 at various time points after infection was examined in order to understand the timing of cleavage events. Cells were infected with GCRV at an MOI of 2.5, and collected at various time points. As shown in Figure 3A, the band of the short polypeptide could be recognized at 9 h p.i., which was earlier than the observed detection time for 1 MOI infection in previous report (Yan et al., 2015). However, the expression of the full-length NS80 protein could be detected at 6 h p.i., which was consistent with previous results (Yan et al., 2015). This observation suggested that the shorter fragment is generated from the cleavage of NS80. To determine the relationship between the amount of the 58-kDa fragment and infection dose, the expression of NS80 in GCRV-infected cells at an MOI of 1.5 was examined (IB data not shown). The relative intensities of the 58-kDa fragment for 3 different MOIs (1, 1.5, and 2.5) were evaluated. As shown in Figure 3B, the relative amount of the 58-kDa fragment was related to infection time and dose. As the infection progressed, the intensity of the 58-kDa polypeptide bands increased slightly 12h p.t., and remained at a stable level 15h p.t.. These results suggested that infection time and dose influence the amount of the 58-kDa fragment of NS80.

The 58-kDa fragment is cleaved from the amino terminus of NS80

To determine whether the short polypeptide was generated by cleavage, rather than via an alternative start codon, recombinant constructs expressing FLAG-tagged NS80 at the N- or C-terminus were constructed. Each of the two plasmids was transfected into BHK cells, and the cell lysates were subjected to an IB analysis with an anti-

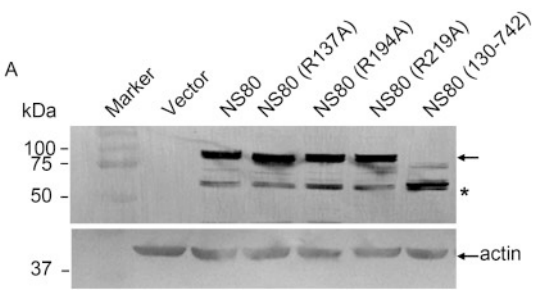

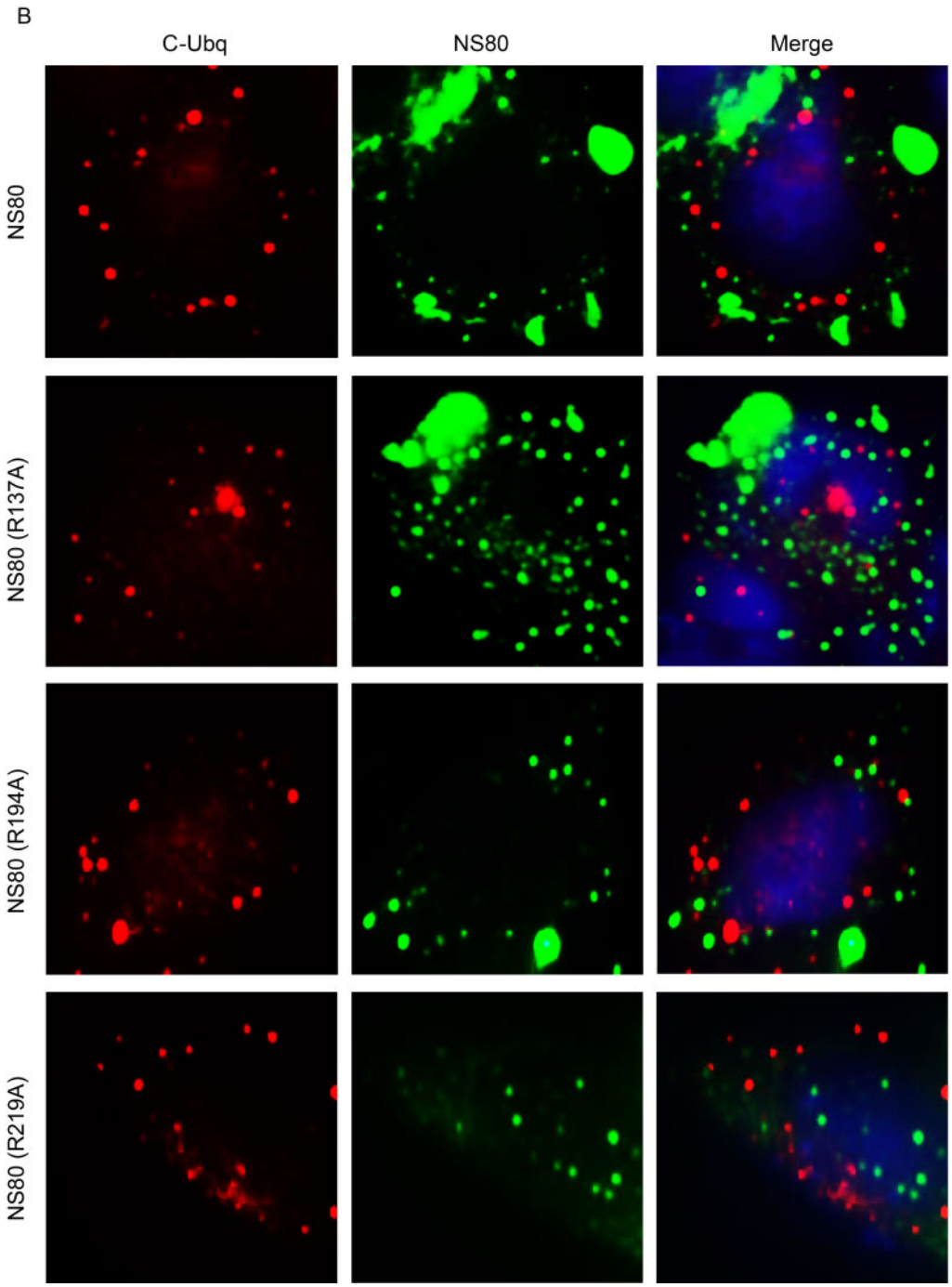

Figure 2. Three mutated protease-sensitive sites are not related to the 58-kDa fragment. (A) Immunoblotting analysis of the expressed mutant NS80 protein. BHK cells were transfected with 4 μg/well pCI-neo empty vector, pCI-neo-NS80, pCI-neo-NS80^{R137A}, pCI-neo-NS80^{R194A}, pCI-neo-NS80^{R219A}, and pCI-neo-NS80 (130–742). Cell lysates were resolved by 10% SDS-PAGE and subjected to an immunoblotting analysis with α-NS80C or β-actin mAb. Arrow indicates the full-length NS80, and the asterisk indicates the 58-kDa NS80 fragment. (B) Ubiquitination analysis of the expressed mutant NS80 protein in transfected cells. Vero cells transfected with plasmids pCI-neo-NS80, pCI-neo-NS80^{R137A}, pCI-neo-NS80^{R194A}, and pCI-neo-NS80^{R219A} were immunostained with α-NS80C and then counterstained with rabbit anti-polyubiquitination pAb, followed by staining with Alexa Fluor® 488 donkey anti-rabbit IgG (Green) and Alexa Fluor® 568 donkey anti-rabbit IgG (red). Nuclei were stained with Hoechst (blue).

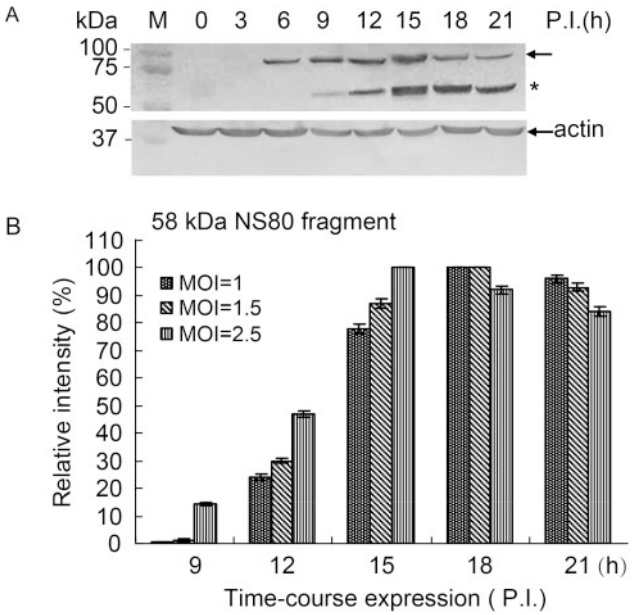

Figure 3. Infection time and dose may influence the amount of the short NS80 fragment. (A) CIK cells infected with GCRV at an MOI of 2.5 were collected at different time points to detect the expression of NS80 by immunoblotting with α-NS80C or β-actin mAb. Arrow indicates the full-length NS80, and the asterisk indicates the 58-kDa NS80 fragment. (B) The relative intensity of the 58-kDa NS80 fragment was quantified using Image J. CIK cells were infected with GCRV at three different MOI (1, 1.5, and 2.5), and the relative intensity of the shorter fragment was determined with respect to β-actin and the maximum value was evaluated.

FLAG mAb. As shown in Figure 4A, using the anti-FLAG mAb, the full-length NS80 and a ~22-kDa protein band were detected when FLAG was tagged at the N-terminus of NS80 (FLAG-NS80), but a ~22 kDa was not found for C-terminal-tagged NS80 (NS80-FLAG), except for the full length NS80 and an approximately 58-kDa protein band. As expected, there were no detectable bands for the expression of non-tagged-NS80 and the empty vector. These results suggested that the 58-kDa fragment is C-terminal NS80, and the 22-kDa fragment might be another product from the N-terminus of NS80.

To further prove that the 58-kDa fragment is cleaved at the N-terminal region of NS80, a specific α-NS80N was generated, as indicated in the Materials and Methods section, and an IB analysis was conducted. As shown in Figure 4B, a ~22-kDa specific band was clearly detected, as was the full-length NS80 and 58-kDa fragment, further indicating that the 58-kDa polypeptide was cleaved from the amino terminus of NS80. Taken together, these results demonstrated that the 58-kDa fragment of NS80 originated from the cleavage of the full-length NS80.

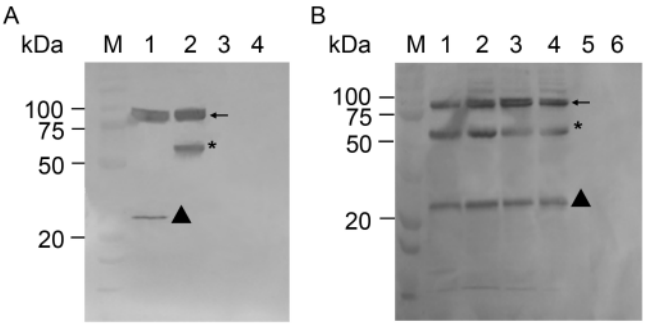

Figure 4. The 58-kDa fragment is cleaved from the amino terminus of NS80. (A) Immunoblotting analysis of NS80 expression in transfected cells with mouse anti-FLAG mAb. M, standard protein marker; Lanes 1–4, BHK cells transfected with pCI-neo-FLAG-NS80 (lane 1), pCI-neo-NS80-FLAG (lane 2), pCI-neo-NS80 (lane 3), and pCI-neo empty vector (lane 4). (B) Immunoblotting analysis of NS80 expression in infected and transfected cells with α-NS80N. M, standard protein marker; Lane 1, GCRV-infected CIK cells; Lanes 2–5, BHK cells transfected with pCI-neo-FLAG-NS80 (lane 2), pCI-neo-NS80-FLAG (lane 3), pCI-neo-NS80 (lane 4), and pCI-neo empty vector (lane 5); Lane 6, mock-infected CIK cells. The arrow indicates the full-length NS80, asterisk indicates the 58-kDa NS80 fragment, and black triangle indicates the 22-kDa fragment.

Subcellular localization of the 58-kDa polypeptide is different from 22-kDa fragment of NS80

The aforementioned results showed that NS80 could be cleaved into two fragments (22 kDa and 58 kDa) in infected and transfected cells. To determine the subcellular localization of the two NS80-related fragments, the localization of the 22-kDa or/and 58-kDa fragments in transfected cells was examined by IF assays with the pCI-neo-NS80 (1–190) plasmid expressing the N-terminal NS80 protein and the pCI-neo-NS80 (386–742) plasmid expressing the C-terminal NS80 protein. As shown in Figure 5A, pCI-neo-NS80 (1–190) exhibited a diffuse subcellular distribution using α-NS80N, while pCI-neo-NS80 (386–742) appeared in typical globular inclusion structures in the cytoplasm using α-NS80C. To confirm the transfection results, the expression of NS80 in infected cells was further examined by IF using α-NS80N and α-NS80C. As shown in Figure 5B, many typical globular inclusion structures were detected in infected cells using both α-NS80N and α-NS80C, but a diffuse subcellular distribution was only detected using α-NS80N. These results suggested that the two cleavage fragments had distinct subcellular localizations, indicating that they might have different functions in viral replication.

In our previous study, we found that NS80 interacts

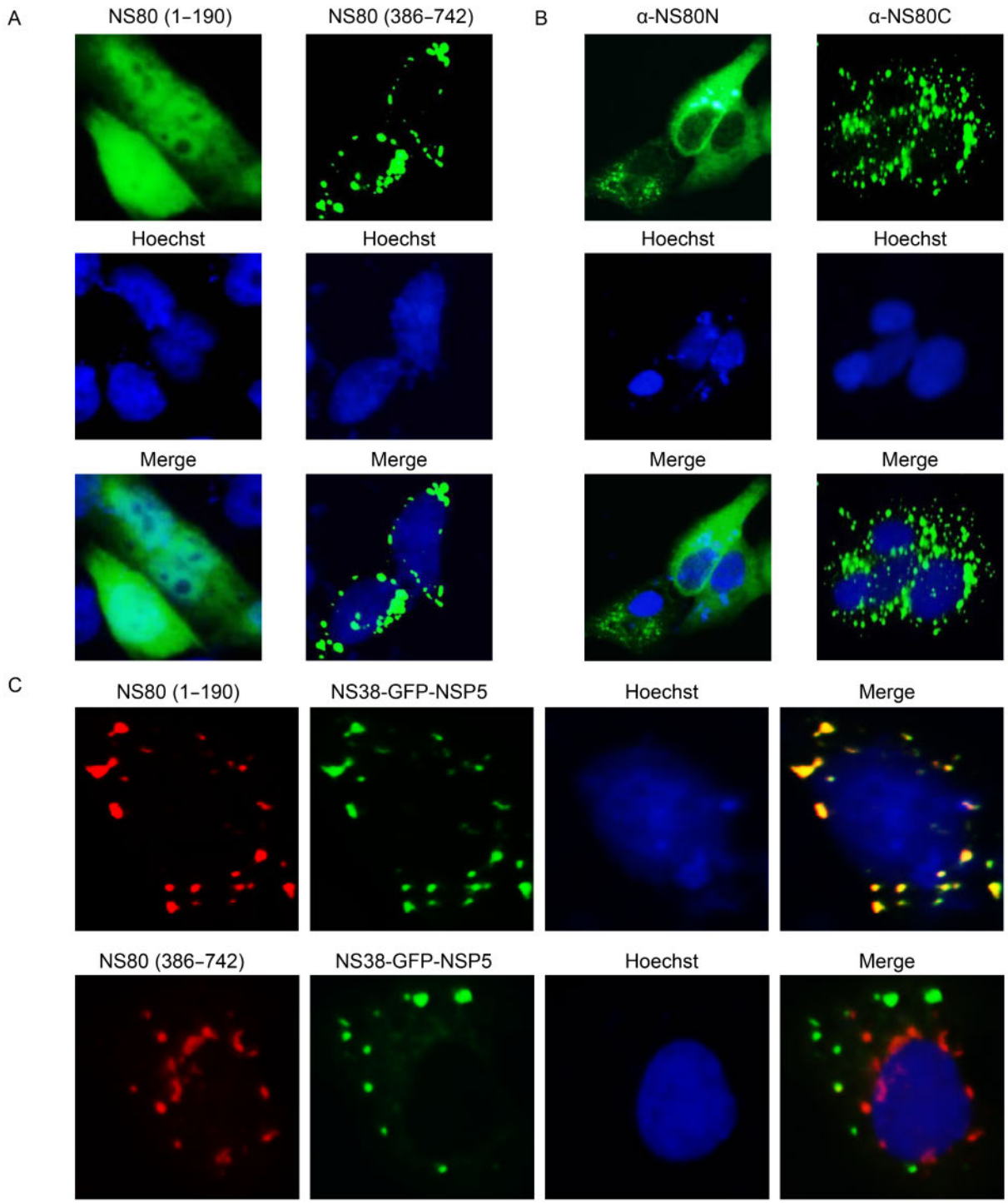

Figure 5. Subcellular localization of the 58-kDa polypeptide is different from that of the 22-kDa fragment of NS80. (A) Vero cells transfected with pCI-neo-NS80 (1–190) or/and pCI-neo-NS80 (386–742) were fixed at 24 h p.t. for immunofluorescence assays with α-NS80N and α-NS80C, respectively, followed by Alexa Fluor® 488 donkey anti-rabbit IgG (Green). Nuclei were stained with Hoechst (blue). (B) FHM cells infected with GCRV were fixed at 12 h p.i. and stained with α-NS80N and α-NS80C, followed by Alexa Fluor® 488 donkey anti-rabbit IgG (Green). Nuclei were stained with Hoechst (blue). (C) Vero cells were co-transfected with NS38-GFP-NSP5 and either pCI-neo-NS80(1–190) or pCI-neo-NS80(386–742). At 24 h p.t., cells were fixed and then stained with α-NS80N and α-NS80C, followed by Alexa Fluor® 568 donkey anti-rabbit IgG (red). Nuclei were stained with Hoechst (blue).

with NS38 in infected and transfected cells (Shao et al., 2013). Additionally, the single rotavirus NSP5 is able to form viral factories in transfected cells (Miller et al., 2010). Accordingly, the NSP5-based protein–protein interaction platform including NS38-GFP-NSP5 was constructed in our lab (Zhang et al., 2016). To further understand whether there is a functional difference between the 22-kDa and 58-kDa fragments of NS80, an association assay was performed using NS38-GFP-NSP5 with the plasmids NS80 (1–190) or/and NS80 (386–742), respectively. As shown in Figure 5C, N-terminal NS80 fully colocalized with NS38-GFP-NSP5, while no association was detected between the C-terminal NS80 and NS38-GFP-NSP5. Therefore, there is an interaction between NS38 and the 22-kDa fragment, but not the 58-kDa fragment. These results demonstrated that the 22-kDa and 58-kDa fragments of NS80 play different roles in viral replication.

DISCUSSION

Previous studies have indicated that reoviruses generate inclusion bodies in the cytoplasm during infection. The nonstructural protein μNS of MRV and its analogue proteins also interact with other viral proteins during infection (Becker et al., 2003; Touris-Otero et al., 2004; Broering et al., 2005; Brandariz-Nunez et al., 2010). These interactions between μNS and multiple viral proteins promote their maintenance within VIBs for efficient viral replication. Recent studies in our lab have indicated that *Aquareovirus* NS80 can induce inclusion structures in infected or transfected cells and interact with other viral proteins (Shao et al., 2013; Yan et al., 2015). In this study, the 58-kDa fragment was identified as an NS80 cleavage product, and may have an important role in viral replication and particle assembly.

Specifically, we detected NS80 and its fragment (approximately 58 kDa) in various infected and transfected cells, and excluded the possibility that the short NS80 fragment was a transient intermediate of protein degradation based on a mutational analysis. In addition, the accumulation of the 58-kDa fragment was related to infection time and dose. Moreover, the short NS80 products were proved to be originated from specific cleavage near the amino terminus of NS80. An approximately 22-kDa fragment was detected using FLAG-tag mAb and α-NS80N. Different subcellular localizations were observed for the 22-kDa and 58-kDa fragments in infected and transfected cells, suggesting that the two fragments have different functions in the viral life cycle. These results strongly suggest the 58-kDa NS80 fragment is a cleavage product, and NS80 may be a multifunctional protein. μNSC in MRV, which lacks the first 40 amino residues of μNS, is also produced naturally during MRV infection (Lee et al., 1981), and its translation is initiated from an alternative site in *M3* mRNA (Busch et al., 2011). Similarly, ARV μNSC was detected in infected cells, but the results of a recent study demonstrated that it originates from a single post-translational cleavage event that occurs near the amino terminus of μNS (Busch et al., 2011). Our results are consistent with these previous results and suggest that the smaller NS80 fragment shares the same post-translational modification mechanism with ARV μNS. Regarding the post-translational modifications, similar observations have been reported for the structural proteins μB and σA in ARV. Both μB and σA can be partially cleaved into two fragments near the amino termini to produce large C-terminal proteins and smaller N-terminal peptides (Varela et al., 1996; Ji et al., 2010). These observations suggest that viruses use a variety of strategies to modify primary translation products for efficient viral replication and particle assembly.

The μNSC of MRV forms inclusion bodies. However, based on RNA interference-based trans-complementation approaches, μNSC is incapable of restoring MRV growth in cultured cells when μNS is absent (Kobayashi et al., 2006; Arnold et al., 2008; Kobayashi et al., 2009). We recently found that the C-terminal region of NS80 is indispensable for VIB formation, and the N-terminal region of *Aquareovirus* NS80 is required for interactions with viral proteins and viral replication (Shao et al., 2013; Zhang et al., 2016); accordingly, the N- and C-terminal regions of NS80 may play different roles in viral replication and particle assembly. In this study, we detected 22-kDa and 58-kDa NS80 fragments, as well as the full-length NS80 with NS80 expression in infected and transfected cells. The 22-kDa N-terminal NS80 showed a diffuse subcellular distribution that differed from the 58-kDa C-terminal NS80 and full-length NS80 phenotypes, suggesting that NS80 presents different forms at different replication stages for efficient replication and assembly in the viral life cycle. The precise cleavage site of the NS80 fragment and the molecular mechanism by which it mediates viral replication are currently under investigation.

In summary, the origin of two NS80 fragments and their related subcellular distributions were investigated. The 58-kDa product was derived from the cleavage of NS80. This cleavage yielded an approximately 58-kDa carboxy-terminal protein and a 22-kDa amino-terminal polypeptide, which exhibited distinct distributions in transfected and infected cells. To our knowledge, this is first study to indicate that the 58-kDa fragment is derived from the cleavage of the NS80 protein. These results contribute to our understanding of the molecular events involving NS80 and the roles of different forms in interactions with other viral or cellular proteins involved

in viral replication and particle assembly.

ACKNOWLEDGMENTS

This work was supported by funding from the National Natural Science Foundation of China (NO. 31372565, 31402340, 31400139 and 31370190).

COMPLIANCE WITH ETHICS GUIDELINES

The authors declare that they have no conflict of interest. This article does not contain any studies with human or animal subjects performed by any of the authors.

AUTHOR CONTRIBUTIONS

QF designed the experiments. QXC, ZJ carried out the experiments. QXC, ZJ, GH, FXZ and QF analyzed the data. QXC, QF wrote the paper. All authors read and approved the final manuscript.

REFERENCES

Arnold MM, Murray KE, Nibert ML. 2008. Formation of the factory matrix is an important, though not a sufficient function of nonstructural protein mu NS during reovirus infection. Virology, 375: 412–423.

Attoui H, Fang Q, Mohd Jaafar F, Cantaloube JF, Biagini P, de Micco P, de Lamballerie X. 2002. Common evolutionary origin of aquareoviruses and orthoreoviruses revealed by genome characterization of Golden shiner reovirus, Grass carp reovirus, Striped bass reovirus and golden ide reovirus (genus Aquareovirus, family Reoviridae). J Gen Virol, 83: 1941–1951.

Becker MM, Peters TR, Dermody TS. 2003. Reovirus sigma NS and mu NS proteins form cytoplasmic inclusion structures in the absence of viral infection. J Virol, 77: 5948–5963.

Brandariz-Nunez A, Menaya-Vargas R, Benavente J, Martinez-Costas J. 2010. Avian reovirus microNS protein forms homo-oligomeric inclusions in a microtubule-independent fashion, which involves specific regions of its C-terminal domain. J Virol, 84: 4289–4301.

Broering TJ, Arnold MM, Miller CL, Hurt JA, Joyce PL, Nibert ML. 2005. Carboxyl-proximal regions of reovirus nonstructural protein muNS necessary and sufficient for forming factory-like inclusions. J Virol, 79: 6194–6206.

Broering TJ, Kim J, Miller CL, Piggott CD, Dinoso JB, Nibert ML, Parker JS. 2004. Reovirus nonstructural protein mu NS recruits viral core surface proteins and entering core particles to factory-like inclusions. J Virol, 78: 1882–1892.

Brookes SM, Hyatt AD, Eaton BT. 1993. Characterization of virus inclusion bodies in bluetongue virus-infected cells. J Gen Virol, 74: 525–530.

Busch LK, Rodriguez-Grille J, Casal JI, Martinez-Costas J, Benavente J. 2011. Avian and mammalian reoviruses use different molecular mechanisms to synthesize their {micro}NS isoforms. J Gen Virol, 92: 2566–2574.

Cai L, Sun X, Shao L, Fang Q. 2011. Functional investigation of grass carp reovirus nonstructural protein NS80. Virol J, 8: 168.

Cheng L, Fang Q, Shah S, Atanasov IC, Zhou ZH. 2008. Subnanometer-resolution structures of the grass carp reovirus core and virion. J Mol Biol, 382: 213–222.

Cheng L, Zhu J, Hui WH, Zhang X, Honig B, Fang Q, Zhou ZH. 2010. Backbone model of an aquareovirus virion by cryo-electron microscopy and bioinformatics. J Mol Biol, 397: 852–863.

Fan C, Fang Q. 2009a. Functional Analyses of Mammalian Reovirus Nonstructural Protein muNS and Expression. Virol Sin, 24: 1–8.

Fan C, Shao L, Fang Q. 2010. Characterization of the nonstructural protein NS80 of grass carp reovirus. Arch Virol, 155: 1755–1763.

Fan C, Zhang L, Lei C, Fang Q. 2009b. Expression and Identification of Inclusion Forming-related Domain of NS80 Nonstructural Protein of Grass Carp Reovirus. Virol Sin, 24: 194–201.

Fang Q, Ke LH, Cai YQ. 1989. Growth characterization and high titre culture of GCHV. Virol Sin, 3: 314–319.

Fang Q, Shah S, Liang Y, Zhou ZH. 2005. 3D reconstruction and capsid protein characterization of grass carp reovirus. Sci China C Life Sci, 48: 593–600.

Fields BN, Raine CS, Baum SG. 1971. Temperature-sensitive mutants of reovirus type 3: defects in viral maturation as studied by immunofluorescence and electron microscopy. Virology, 43: 569–578.

Guo H, Sun X, Yan L, Shao L, Fang Q. 2013. The NS16 protein of aquareovirus-C is a fusion-associated small transmembrane (FAST) protein, and its activity can be enhanced by the nonstructural protein NS26. Virus Res, 171: 129–137.

Ivanovic T, Boulant S, Ehrlich M, Demidenko AA, Arnold MM, Kirchhausen T, Nibert ML. 2011. Recruitment of cellular clathrin to viral factories and disruption of clathrin-dependent trafficking. Traffic, 12: 1179–1195.

Ji WT, Lin FL, Wang YC, Shih WL, Lee LH, Liu HJ. 2010. Intracellular cleavage of sigmaA protein of avian reovirus. Virus Res, 149: 71–77.

Kobayashi T, Chappell JD, Danthi P, Dermody TS. 2006. Gene-specific inhibition of reovirus replication by RNA interference. J Virol, 80: 9053–9063.

Kobayashi T, Ooms LS, Chappell JD, Dermody TS. 2009. Identification of functional domains in reovirus replication proteins muNS and mu2. J Virol, 83: 2892–2906.

Lee PW, Hayes EC, Joklik WK. 1981. Characterization of anti-reovirus immunoglobulins secreted by cloned hybridoma cell lines. Virology, 108: 134–146.

Mertens P, Attoui H, Duncan R, Dermody T, et al. 2011. The Double Stranded RNA viruses. In Virus Taxonomy. Ninth Report of the International Committee on Taxonomy of Viruses. Edited by Andrew MQ King, Adams Michael J, Carstens Eric B, Lefkowitz Elliot J. Oxford: Elsevier: 497–650.

Miller CL, Broering TJ, Parker JS, Arnold MM, Nibert ML. 2003. Reovirus sigma NS protein localizes to inclusions through an association requiring the mu NS amino terminus. J Virol, 77: 4566–4576.

Miller CL, Arnold MM, Broering TJ, Hastings CE, Nibert ML. 2010. Localization of mammalian orthoreovirus proteins to cytoplasmic factory-like structures via nonoverlapping regions of microNS. J Virol, 84: 867–882.

Parker JS, Broering TJ, Kim J, Higgins DE, Nibert ML. 2002. Reovirus core protein mu2 determines the filamentous morphology of viral inclusion bodies by interacting with and stabilizing microtubules. J Virol, 76: 4483–4496.

Rangel AA, Rockemann DD, Hetrick FM, Samal SK. 1999. Identification of grass carp haemorrhage virus as a new genogroup of aquareovirus. J Gen Virol, 80: 2399–2402.

Shao L, Fan C, Maj E, Fang Q. 2010. Molecular characterization of nonstructural protein NS38 of grass carp reovirus. Virol Sin, 25: 123–129.

Shao L, Guo H, Yan LM, Liu H, Fang Q. 2013. Aquareovirus NS80 recruits viral proteins to its inclusions, and its C-terminal domain is the primary driving force for viral inclusion formation. PLoS One, 8: e55334.

Sharpe AH, Chen LB, Fields B N. 1982. The interaction of mammalian reoviruses with the cytoskeleton of monkey kidney CV-1 cells. Virology, 120: 399–411.

Shaw AL, Samal SK, Subramanian K, Prasad BV. 1996. The structure of aquareovirus shows how the different geometries of the two layers of the capsid are reconciled to provide symmetrical interactions and stabilization. Structure, 4: 957–967.

Silverstein SC, Schur PH. 1970. Immunofluorescent localization of double-stranded RNA in reovirus-infected cells. Virology, 41: 564–566.

Smith RE, Furuichi Y. 1980. Gene mapping of cytoplasmic polyhedrosis virus of silkworm by the full-length mRNA prepared under optimized conditions of transcription in vitro. Virology, 103: 279–290.

Touris-Otero F, Martinez-Costas J, Vakharia VN, Benavente J. 2004. Avian reovirus nonstructural protein microNS forms viroplasm-like inclusions and recruits protein sigmaNS to these structures. Virology, 319: 94–106.

Varela R, Martinez-Costas J, Mallo M, Benavente J. 1996. Intracellular posttranslational modifications of S1133 avian reovirus proteins. J Virol, 70: 2974–2981.

Wiener JR, Bartlett JA, Joklik WK. 1989. The sequences of reovirus serotype 3 genome segments M1 and M3 encoding the minor protein mu 2 and the major nonstructural protein mu NS, respectively. Virology, 169: 293–304.

Yan L, Liu H, Li X, Fang Q. 2014. The VP2 protein of grass carp reovirus (GCRV) expressed in a baculovirus exhibits RNA polymerase activity. Virol Sin, 29: 86–93.

Yan L, Zhang J, Guo H, Yan S, Chen Q, Zhang F, Fang Q. 2015. Aquareovirus NS80 initiates efficient viral replication by retaining core proteins within replication-associated viral inclusion bodies. PLoS One, 10: e0126127.

Yang C, Ji G, Liu H, Zhang K, Liu G, Sun F, Zhu P, Cheng L. 2012. Cryo-EM structure of a transcribing cypovirus. Proc Natl Acad Sci U S A, 109: 6118–6123.

Zhang J, Guo H, Chen Q, Zhang F, Fang Q. 2016. The N-Terminal of aquareovirus NS80 is required for interacting with viral proteins and viral replication. PLoS One, 11: e0148550.

Zhang X, Jin L, Fang Q, Hui WH, Zhou ZH. 2010. 3.3 A cryo-EM structure of a nonenveloped virus reveals a priming mechanism for cell entry. Cell, 141: 472–482.